Effect of temperature and SiO_2 nanoparticle size on wettability alteration of oil-wet calcite

Effect of temperature and SiO_2 nanoparticle size on wettability alteration of oil-wet calcite

Sarmad Al-Anssari[a, b*], Shaobin Wang[a], Ahmed Barifcani[a, c], Maxim Lebedev[d], Stefan Iglauer[c]

[a]*Department of Chemical Engineering, Curtin University, Kent Street, 6102 Bentley, Australia*
[b]*Department of Chemical Engineering, University of Baghdad, Iraq*
[c]*Department of Petroleum Engineering, Curtin University, 26 Dick Perry Avenue, 6151 Kensington, Australia*
[d]*Department of Exploration Geophysics, Curtin University, 26 Dick Perry Avenue, 6151 Kensington, Australia*
[*]corresponding author

Abstract

Nanofluid treatment of oil reservoirs is being developed to enhance oil recovery and increase residual trapping capacities of CO_2 at the reservoir scale. Recent studies have demonstrated good potential for silica nanoparticles for enhanced oil recovery (EOR) at ambient conditions. Nanofluid composition and exposure time have shown significant effects on the efficiency of EOR. However, there is a serious lack of information regarding the influence of temperature on nanofluid performance; thus the effects of temperature, exposure time and particle size on wettability alteration of oil-wet calcite surface were comprehensively investigated; moreover, the stability of the nanofluids was examined. We found that nanofluid treatment is more efficient at elevated temperatures, while nanoparticle size had no influence. Mechanistically most nanoparticles were irreversibly adsorbed by the calcite surface. We conclude that such nano-formulations are potentially useful EOR agents and may improve the efficiency of CO_2-storage even at higher reservoir temperatures.

Keywords: Wettability alteration, Carbonate reservoirs, EOR, Oil-wet, Nanoparticles, Silicon dioxide, Temperature, Zeta potential.

1. Introduction

Nanoparticles with unique designed properties are an elegant solution for many industrial problems and they have ubiquitous promising application in numerous fields ranging from medicine [1] and biomedicine [2], drug delivery [3], biology [4, 5], environment [6] and pollution [7, 8], water treatment [9, 10], food production [11-13], polymer composite [14], stable emulsions [15, 16], heat transfer [17, 18], corrosion protection [19], conductive materials [20], heterogeneous catalysis [21], and subsurface applications including drilling [22], carbon geosequestration [23, 24] and enhanced oil recovery [23, 25-27]. Deposition of (functionalized) nanoparticles on the solid surfaces is a promising technique to control the wettability of these surfaces.

The efficiency of nanoparticles in terms of wettability alteration of solid surfaces depends on several factors including particularly the nanoparticle type [28, 29] and solid surface chemistry [30]. Also, operating conditions such as nanofluid composition and contact time have significant effects on such surface modifications [23, 31]. A major challenge in enhanced oil recovery (EOR), on which we focus here, is hydrocarbon production from naturally fractured carbonate reservoirs; oil production here is controlled by imbibition of water into the oil-wet rock matrix. Currently, these typically oil-wet and intermediate-wet reservoirs account for more than half of the known remaining oil in the world [32-34]. As most oil is stored in the matrix [35], water during secondary recovery can only move through fractures, resulting in the low productivity (10-30%) of oil by water flooding [36, 37]. Alteration of oil-wet carbonate surfaces to water-wet is thus a key mechanism, which can significantly increase oil production [23, 27, 38-43]. Once wettability is altered to water-wet, water can imbibe into the matrix of the rock and displace a significantly higher ratio of oil from the pore space [44].

Water-wet reservoirs are also favourable to carbon capture and storage (CCS), Iglauer et al. [45], specifically structural [46, 47] and residual [48] trapping capacities are significantly lower in oil-wet formations. It is thus desirable to render oil-wet reservoirs water-wet to optimize CCs projects.

Previous investigations have studied the application of nanoparticles for EOR in sandstone reservoirs [25, 38, 42, 49, 50]; however, only limited information is available in terms of the activity of silicon dioxide nanoparticles to improve oil displacement efficiency in carbonate reservoirs. Specifically, Karimi et al. [41] and Nwidee et al. [43] have examined the role of ZrO_2 nanoparticles on wettability alteration of carbonate reservoirs using contact angle (θ) measurements. They showed that ZrO_2-based nanofluids can significantly alter strongly oil-wet rocks to water-wet. Bayat et al. [28] studied the influence of several types of nanoparticles including, aluminium oxide (Al_2O_3), titanium oxide (TiO_2), and silicon dioxide (SiO_2) on the production of oil from limestone reservoirs. It was found that SiO_2 nanoparticles are more efficient than TiO_2 and Al_2O_3 regarding wettability alteration towards a more water-wet state. Similarly, Moghaddam et al. [29] conducted a comparative study using different types of nanoparticles including magnesium oxide (MgO), cerium oxide (CeO_2), carbon nanotubes (CNT) as well as all types previously studied by Bayat et al. [28]. The results of contact angle, imbibition and core flooding experiments at room temperature revealed that SiO_2 nanoparticles are more effective in wettability alteration and improved oil recovery. Lately, the effect of silica nanofluid on carbonate surfaces wettability was also investigated by Al-Anssari et al. [23] concerning nanofluid composition (brine and nanoparticles concentrations), immersion time and reversibility of nanoparticle adsorption. Their results showed that at room conditions, silica nanoparticles can render the strongly oil-wet surface water-wet. Furthermore, Zhang et al. [27] have conducted contact angle and core flooding experiments with silica nanofluid at room temperature. A high resolution X-ray microtomography (micro CT) was used to image oil and brine distribution in the core before and after nanofluid flooding. Their results confirmed the effect of silica nanoparticles on surface wettability and demonstrated that approximately 15% more oil can be produced using silica nanofluid.

At harsh reservoirs conditions, particularly at high temperature and salinity, the fluids chemistry plays a crucial role in surfaces wettability [35, 51, 52] and nanofluid stability [53-55], leading to aggregation and sedimentation of nanoparticles owing to significant reduction in zeta potential (ζ). However, the effect of salinity and particularly temperature on nanofluid stability and ability to render oil-wet surfaces water-wet are only poorly understood.

In this work, we thus investigate how temperature and nanoparticle size affect nanofluid wettability alteration of intermediate-wet and oil-wet calcite surfaces. Moreover, zeta potentials for nanofluids of different compositions was measured, and the phase behaviour of the prepared nanofluid was monitored.

2. Experimental Methodology

2.1. Materials

Iceland spar (pure calcite, from WARD'S Natural Science) was used as a representative for carbonate reservoir rock. Atomic force microscopy (model DSE 95-200) was used to measure the topography of the calcite samples since wettability [56] and rate of nanoparticle adsorption are controlled by the surface roughness and nanoparticles distribution [57]. The root mean square (RMS) surface roughness ranged between 18-32 nm, which is very smooth.

n-decane (>99 mol%, Sigma-Aldrich) was used as model oil. Toluene (99mol%, Chem-supply), n-hexane (>95 mol%, Sigma-Aldrich), nitrogen (>99.99 mol%, BOC), acetone and methanol (99.9 mol%, Rowe Scientific) were used as cleaning agents. Sodium chloride (≥99.5 mol%, Scharlan) was used to prepare brine solutions. Silicon dioxide nanoparticles (porous spherical, purity = 99.5 wt%, Sigma Aldrich) with two different sizes (5-10 nm and 20-25 nm) were used separately to prepare nanofluids with different particle sizes (Table 1). Deionized (DI) water (Ultrapure from David Gray; conductivity = 0.02 mS/cm) was used to prepare brines or nanofluid (base fluid). Calcite carbonate powder (ACS reagent, ≥99.0%, Sigma-Aldrich) was used to establish an accurate equilibrium between calcite mineral and surrounding electrolyte. The silica nanoparticles were sonicated with base fluid (DI water or brine) to prepare nanofluids; details about the preparation process are described by Al-Anssari et al. [23] and Nwidee et al. [43].

Stearic acid (≥98.5%, Sigma Aldrich) was used to render the original calcite surface (which is strongly water-wet, see below) oil-wet.

Table 1: Properties of silicon dioxide nanoparticles (Sigma Aldrich 2015).

Purity (wt%)	99.5
Density (kg/m^3)	(2200-2600)
Boiling point (K)	2503
Melting point (K)	1873
Molecular mass (g/mole)	60.08
Solubility in water	Insoluble

2.2. Calcite surface preparation

Cleaning steps are crucial in contact angle measurements as residual contaminations can lead to systematic errors [58]. Therefore, the calcite samples were first flushed with ultra clean air to remove any loose calcite, followed by washing with DI water and rinsed with toluene to remove any organic and inorganic contaminants. Note that the DI water and brines used in this study was equilibrated with $CaCO_3$ to avoid a dramatic surface dissolution [59]. Experimentally, different amounts of calcite carbonate powder (ACS reagent, ≥99.0%, Sigma-Aldrich) have been efficiently mixed with several brine samples for 2h. Then all samples had left for a week to monitor if any precipitation of calcite occur. Thus the sample with highest powder load without showing any precipitation of solid particles have been used as an equilibrated brine. Subsequently, cleaned calcite samples were dried for 60 min at 100°C and exposed to air plasma for 40 min (using a Diemer Yocto instrument) to further remove any residual contaminants [23, 58]. Modification of calcite surface with stearic acid (see below for detailed protocol) was started immediately after surface preparation.

2.3. Contact angle measurements

In order to investigate the efficiency of nanofluids in terms of wettability alteration, the contact angle of water droplet on a different calcite surfaces in n-decane was measured. The tilting-plate technique [60] was used to measure advancing (θ_a) and receding (θ_r) water contact angles. A 6-7 µL water drop was dispensed onto the calcite substrate that was placed on a metal platform at an inclination angle of 17° [23, 47]. The water contact angles were measured just before the drop started to slide. A high resolution video camera (Basler scA 640–70 fm, pixel size = 7.4 µm; frame rate = 71 fps; Fujinon CCTV lens: HF35HA-1B; 1:1.6/35 mm) was used to record movies of these whole processes, and θ_a and θ_r were measured on images extracted from the movie files. The percentage error of contact angle measurement was ±3%. Initially the pure calcite surface was tested in air and $\theta_a = \theta_r = 0°$ (completely water-wet).

2.4. Calcite modification with stearic acid

Subsequently the calcite surfaces were rendered oil-wet by following process: stearic acid ($CH_3(CH_2)_{16}COOH$) was initially dissolved in n-decane to prepare a 0.01M stearic acid solution. Here, stearic acid was initially formulated by dissolving 0.285 g of stearic acid in 100 mL of n-decane (>99 mol%, Sigma-Aldrich) with mixing by a magnetic stirrer for a sufficient time. Stearic acid as a long chain fatty acid can actively adsorbs on the calcite surface rendering it to oil or strongly oil-wet [61-63]. The calcite substrate was first immersed in low pH aqueous solution (1 wt% NaCl, pH=4) for 30 min to allow water to diffuse into the lattice of the water-wet sample. A 1/5 weight ratio for solid sample to aqueous solution was used [64]; pH values of this aqueous solution were regulated with drops of HCl and NaOH. Air was then carefully blown over the calcite surface to remove the surface water film. Then, the calcite sample was immersed directly into the 0.01M stearic acid/n-decane solution and aged at ambient condition for 24 h.

$$CaCO_3 + H_2O \leftrightarrow Ca^{2+} + HCO_3^- + OH^- \qquad (1)$$

$$CH_3(CH_2)_{16}COOH \leftrightarrow CH_3(CH_2)_{16}COO^- + H^+ \qquad (2)$$

$$Ca^{2+} + 2(CH_3(CH_2)_{16}COO^-) \leftrightarrow Ca(CH_3(CH_2)_{16}COO)_2 \qquad (3)$$

Ionization of carboxylic acid groups on the calcite surface depends on the ionic strength of the aqueous phase (water composition, Hoeiland et al. [65]). Moreover, it is well established that the surface potential determining ions of calcite in contact with an aqueous phase are Ca^{2+}, CO_3^{2-}, HCO_3^-, and $CaHCO_3^+$. Thus the distribution of these potential-determining ions controls the surface charge and therefore the zeta potential of calcite. Note that $H^+$and OH^- ions are only of secondary importance in terms of the surface potential, particularly at pH 6 to 11[66, 67]. Experimentally, we thus used an acidic aqueous phase (pH= 4) to assure a distinctive positive charge on the calcite surface before aging with stearic acid [61]. This procedure thus accelerates the aging and better mimics reservoir conditions where formation fluids are exposed to the surface over geological times.

Note that in all previous studies, calcite samples were directly aged in stearic acid solution after immersing in water without air drying [61, 68, 69]. However, we found that the presence of a notable water film on the calcite surface prior to immersion into stearic acid solution leads to unstable θ measurements. This phenomenon is owing to the instability of the water film covering the mineral surface [65].

2.5. Nanofluid preparation

Nanofluids were formulated by sonicating silicon dioxide nanoparticles (properties are listed in Table 1) in base fluid (equilibrated DI water or brine) using an ultrasonic homogenizer (300 VT Ultrasonic Homogenizer/ BIOLOGICS) for 20 min. Considering our earlier work on nanofluids [23] and the observations from ShamsiJazeyi et al. [14] with respect to the (detrimental) effects of high nanoparticle concentration on rock permeability, we used a low SiO_2 nanoparticle concentration (0.2 wt%) in a different equilibrated brines (0 - 2 wt% NaCl). The nanofluid was sonicated 4 times at 240 W for 5 min with 5 min rest to avoid overheating. Finally, the prepared nanofluid was stored in a cold and dark for 2 h to assure homogeneity and stability.

2.6. Zeta potential measurements and stability of nanofluids

Zeta potentials (ζ) of the nanofluids were measured using a Zetasizer Nano ZS instrument (Malvern Instruments, UK). Specifically, the zeta potential was obtained from electrophoretic mobility measurements and application of the Smoluchowski-Helmholtz equation:

$$\xi = (\varepsilon . \mu_E)/\mu$$

where ζ is the zeta potential (mV), ε is the dielectric constant of the solution, μ_E is the electrophoretic mobility (equal to V_E/E); V_E is the electrophoretic rate (s^{-1}), E is the electric field ($V.m^{-1}$), and μ is the fluid viscosity. The effect of fluid pH and nanofluid composition on zeta potential was measured systematically as part of this study.

2.7. Calcite wettability modification with silica nanofluid (nano-modification)

In order to investigate the effect of temperature and nanoparticle size on nanofluid efficiency in terms of wettability alteration, oil-wet calcite samples were immersed in nanofluids at different temperatures (23, 30, 40, 50, and 60°C) for different immersing times (15, 30, 45, 60, 90, 120, 180, and 240 min). Specifically, the clean oil-wet substrates were placed in a glass container and were entirely submerged in nanofluid. The calcite samples were laid vertically in the nanofluids to avoid the effect of nanoparticle deposition by gravity. Thus, changes in wettability are solely caused by adsorption of nanoparticles onto the calcite surface. A constant immersion ratio of 5g nanofluid and 1g of calcite was used. The sample container was kept away from light to avoid any degradation effects during modification. After the prescribed immersion time, the sample was removed from the container and flushed with acetone and DI water, then dried with ultrapure nitrogen. Two sets of experiments were performed regarding the temperature effect; in the first set (A) samples were immersed at 23°C, while contact angle measurements were conducted at specified elevated temperatures. In the second set (B), both immersion and contact angle measurements were carried out at the same (elevated) temperature.

3. Results and discussions

Oil production from fractured oil-wet carbonate formations, can be significantly increased by shifting the rock surface wettability from oil-wet to water-wet [34, 38, 49]. Moreover, if the rock is strongly water-wet, the trapping capacity of CO_2 is significantly higher [45-48]. In this context it has been shown that nanofluids have a drastic ability to render oil-wet carbonate surface water-wet [23, 27, 29, 43]. However, the effect of temperature and nanoparticle size has not been systematically studied yet. We thus systematically analysed the effect of these parameters on wettability alteration efficiency.

3.1. Zeta potential of nanofluids

The nanofluids zeta potential has a direct relationship with suspension stability as well as the adhesion and wetting phenomena [70]. Nanoparticles with lower zeta potentials are electrically more unstable and thus flocculate and precipitate more rapidly [71]. Stability of nanofluid is an essential parameter that can limit the nanofluid application, and it depends on both the van der Waals attraction [70] and electrostatic repulsion forces among nanoparticles [31]. Hydrocarbon reservoirs usually contain relatively high salt concentrations and thus the effect of NaCl concentration on suspension stability was investigated. The standard deviation of measurements was varied depending on suspensions salinity and distances from the isoelectric point (IEP); the point at which zeta potential equals zero.

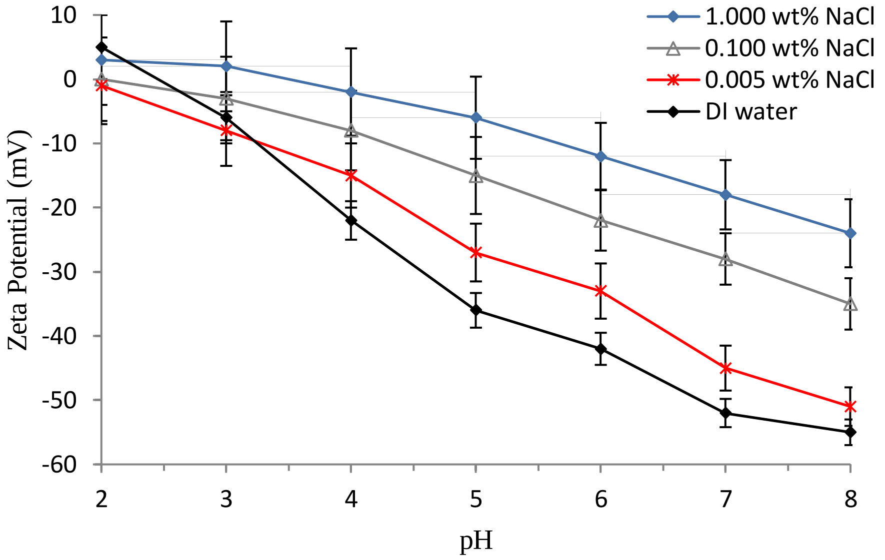

Fig. 1. Zeta potentials of various SiO_2 nanofluids (0.2 wt% SiO_2 in different brine) at varying pH and 23 °C.

Figure 1 shows the variation of zeta potential with pH of silica nanoparticle suspensions at different salinity. The absolute value of zeta potential (ζ) increased with pH and decreased with salinity consistent with literature data for ($\leq$ 0.01 wt% NaCl) [28, 72]. Electrolyte ions reduce the repulsion force among nanoparticles owing to the neutralization of particle surface charges. According to DLVO (Deriaguin-Landan-Verway and Overbeek) theory, attraction and repulsion forces among particles depend on the surface electric charge; thus, the stability of colloidal suspension in a dielectric medium is determined by the repulsive electrostatic interaction energy and attraction of van der Waals energy which is affected by salt concentration. Consequently, higher ionic strength leads to nanoparticles instability due to the lower zeta potential. Note that the formation of salt bridges among silica nanoparticles [73, 74] is the main reason for the instability of nanofluid suspension.

Furthermore, particle loading affects the zeta potential, Figure 2

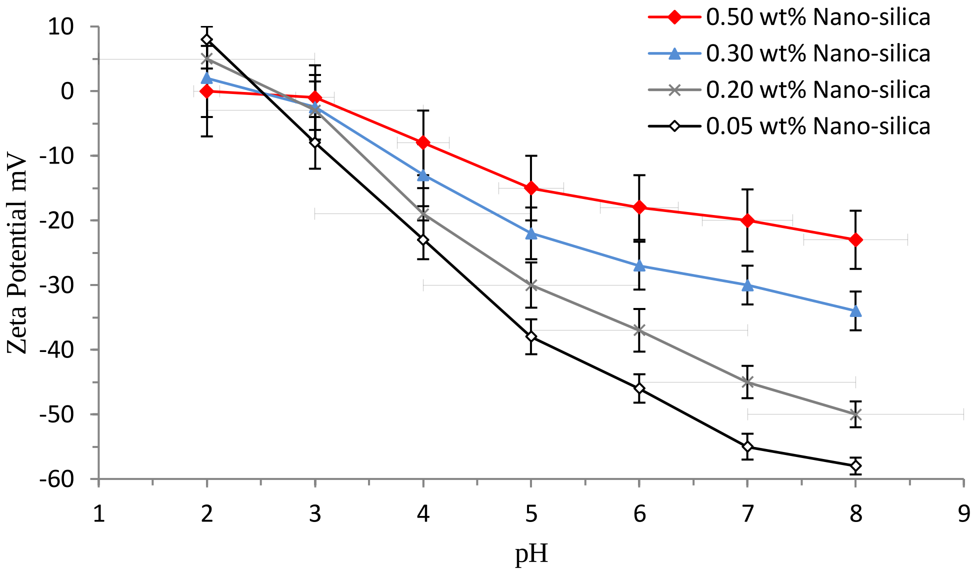

Fig. 2. Zeta potential of various nanofluids with different particle loading (0.05, 0.1, 0.15, 0.2, 0.4 and 0.5 wt% SiO_2in DI water) at varying pH and 23 °C.

The absolute value of zeta potential increased with pH and decreased as particle concentration increased. At low particle loading (≤ 0.2 wt% SiO_2), the increase in nanoparticle concentration had only a small influence; however, at higher particle content, the increase in particle concentration remarkably decreased the absolute value of the zeta potential. This is different to Tantra et al. [54] who claim that only within very low zeta potential (10^{-2}-10^{-4}), the zeta potential is not a function of nanoparticle loading. Consequently, at high nanoparticle load, it is necessary to increase the pH of the suspension to keep the nanofluid far away from the isoelectric point (IEP): the point at which zeta potential of the suspension equals zero [75], as then the nanofluid rapidly flocculated.

The (0.2 wt% SiO_2 in 1 wt% NaCl) nanofluid showed stable behaviour during the investigation period. Note that Franks [76] found that silica nano-suspensions are stable against agglomeration and sedimentation even at relatively high salt concentration (≤ 6 wt % NaCl) if the pH of the solution is kept at an appropriate value. Thus, all prepared nanofluids were kept at pH 5-6 to ensure stability.

3.2. SEM-EDS and AFM analysis

The irreversibly adsorbed fraction of nanoparticles (i.e. after the nano-treated substrate was exposed to different cleaning fluids) was investigated via scanning electron microscopy (SEM, Zeiss Neon 40EsB FIBSEM), energy dispersive X-ray spectroscopy (EDS, Oxford X-act SSD X-ray detector with Inca and Aztec software), and atomic force microscopy AFM instruments (model DSE 95-200, semilab). EDS indicated a significant concentration of silicon (~ 2 wt%) on five different points on several samples (which were treated by nanofluids at various temperatures), Tables 2 and 3. Note that values on Table 3 are average values for measurements taken from five different points in each sample. Although Ma et al. [67] announced that it is challenging to determine the complicated surface charges of carbonate due to the effect of small impurities (e.g. aluminium (Al), and silicon (Si)) on zeta potential, X-ray photoelectron spectroscopy (XPS) showed that calcite samples was totally made of calcium (Ca). Surfaces charge difference between calcite and silica nanoparticle is the main motive force for nanoparticles adsorption on calcite [31]. Mechanistically, negatively-charged silica nanoparticles are strongly adsorbed onto the positively-charged calcium ions of calcite. The electrokinetic data showed that the isoelectric points of calcite were at a pH ranged from (7.8 to 10.6) depending on the ionic strength in aqueous solutions [77]. Thus, calcite surface becomes positively charged when it came into contact with nanoparticles from stable silica nanofluid at pH=5-6 [53]and nanoparticles were adsorbed homogeneously on all surfaces at all temperatures, consistent with previous results [23] at room temperature and other glass and silicon substrates [19, 78].

The calcite surface significantly changed after nanofluid exposure, nanoparticles irregularly spread on the surface (Fig. 3-A and B) while an increase in immersion temperature changed the form and structure of the surface (Fig. 3-C and D); e.g. a temperature increase from 23 to 50 °C increased the adsorption of nanoparticles on the solid surface and enlarged the size of silica agglomerates into larger clusters (Fig. 3-E and F).

AFM measurements performed on the nano-modified calcite surfaces confirmed the observations (Fig.4). Treating calcite with nanofluid increased the surface roughness (Fig. 4 B) and higher surface roughness was measured for higher immersion temperatures (Fig. 4 C). The root-mean-square (RMS) surface roughness increased from 18-32 nm for the original calcite surface to 450-580 nm when treated at room temperature and a maximum 2100- 2700 nm when the surface was treated at higher temperature (60°C).

Table 2: Surface composition, measured by EDS, of oil-wet calcite after modification with nanofluid at 40 °C (0.2 wt% SiO_2 in 1 wt% NaCl brine, 1 h exposure time).

Point	Calcium (wt%)	Silicon (wt%)	Oxygen (wt%)
1	33.1	2.2	64.7
2	34.2	1.9	63.9
3	33.2	2.7	64.1
4	35.1	1.8	63.1
5	32.7	2.5	64.8

Table 3: Surface composition of the oil-wet calcite after modification with nanofluid at (0.2 wt% SiO_2 in 1 wt% NaCl brine, 1 h exposure time) at different temperatures; note that the composition given for each temperature is the average value of five measurements.

Sample	Temperature (°C)	Calcium (wt%)	Silicon (wt%)	Oxygen (wt%)
1	23	34.2	1.2	64.6
2	30	34.3	1.9	63.8
3	40	34.2	2.5	63.3
4	50	35.1	2.2	62.7
5	60	34.4	2.1	63.5

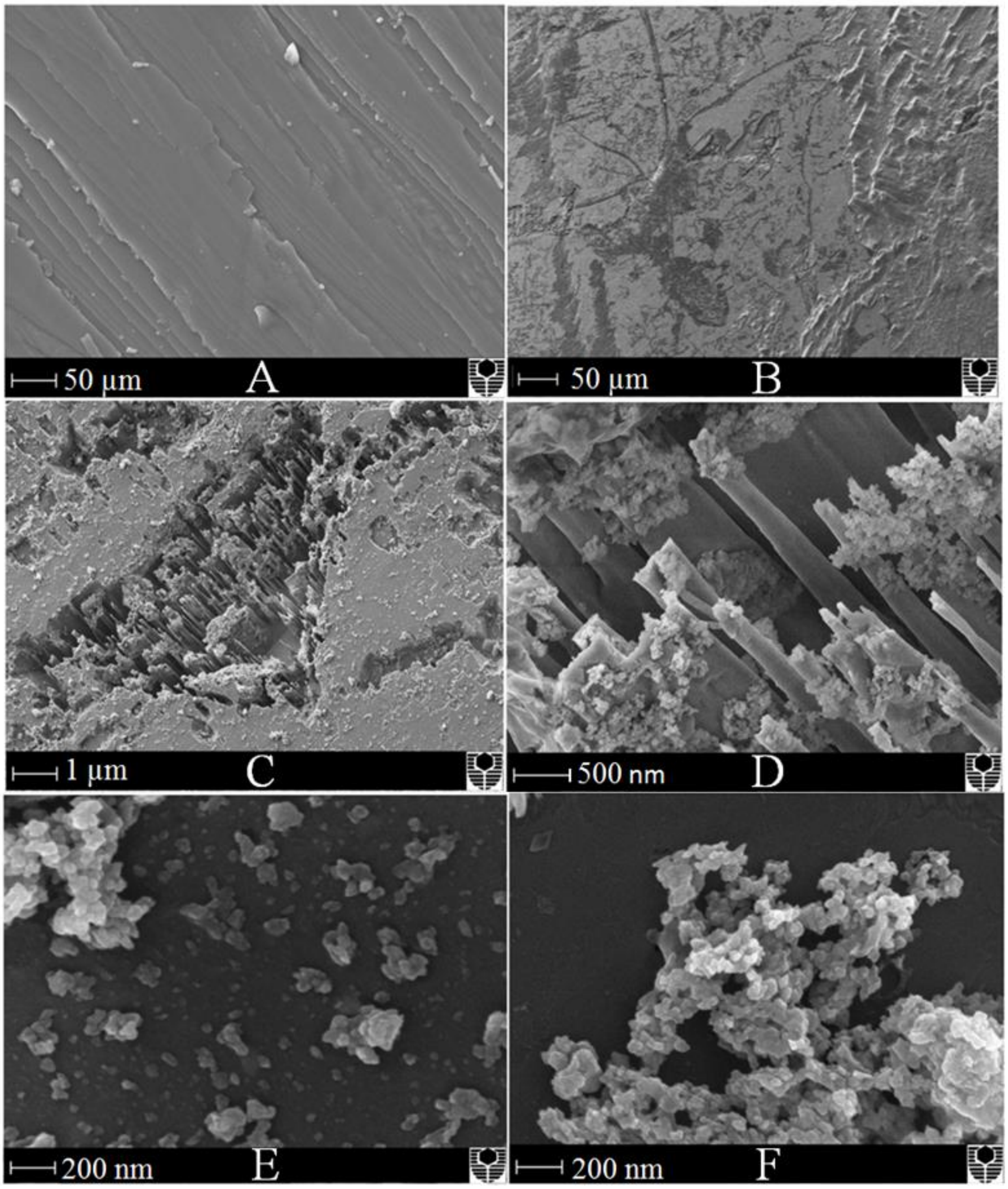

Fig. 3. SEM images of an oil-wet calcite surface: (A) before, (B) after nanofluid treatment (0.2 wt% SiO_2 in 1 wt% NaCl brine) at 23 °C; (C and D) effect of temperature increase on surface morphology; (E and F) maximum resolution zoom-into the irreversibly adsorbed silica agglomerates at 23° (left) and 50 °C (right), respectively.

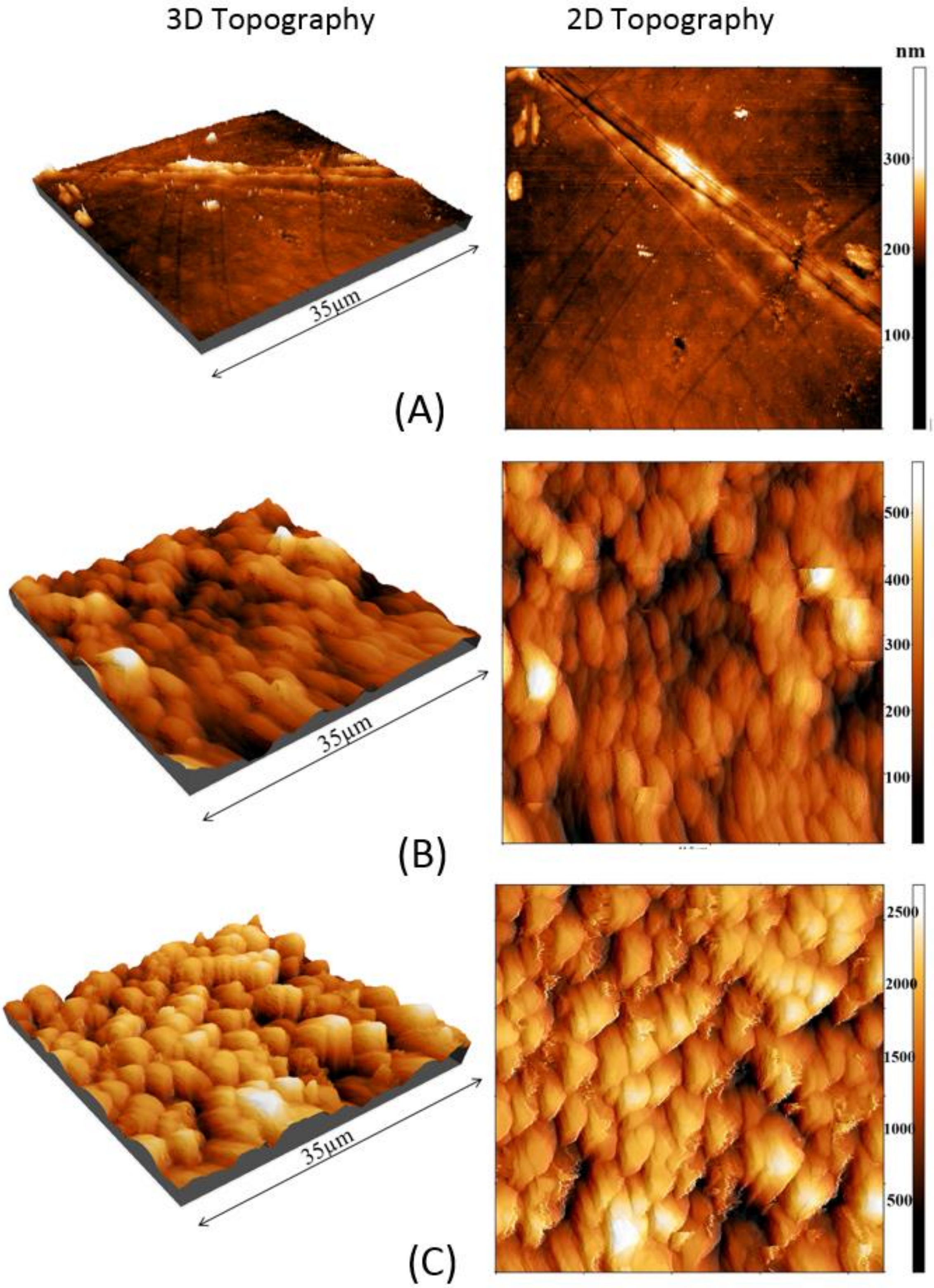

Fig. 4. Atomic force microscopy images of a calcite surface used in the experiment before (A) and after nano-treatment at two different temperatures: 23 °C (B) and 60 °C (C).

3.3. Effect of particles size on wettability alteration.

All oil-wet samples were immersed in an equilibrated brine of the same composition as that used in nanofluid preparation, and contact angles were recorded as a base contact angle before nano-treatment. Thus, θ reduction after treatment with nanofluid was related only to the effect of nanoparticles rather than the effect of the base fluid.

Two SiO_2 nanoparticle sizes (5 and 25 nm) were used to formulate two distinct nanofluids (but with the same concentration 0.2 wt% SiO_2 in 1wt % NaCl brine).

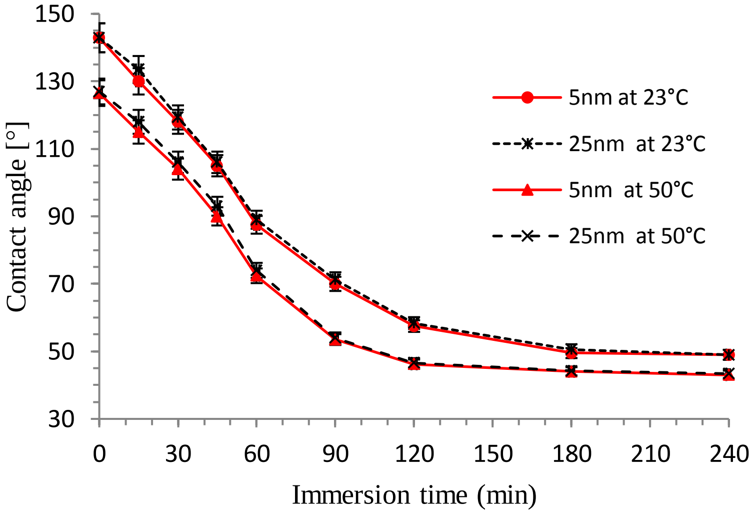

Fig. 5. Water advancing contact angle on oil-wet calcite surface in n-decane as a function of exposure time to nanofluid (0.2wt % SiO_2, 1wt % NaCl brine), temperature (23 and 50°C), and nanoparticle size (5 nm and 25 nm).

Initially the water advancing contact angles in decane at 23 °C and 50 °C measured θ = 144 ±2° and 126 ±2°, respectively, on the untreated surface, which indicates an oil-wet condition. After immersing the oil-wet substrate in silica nanofluid for 2 h at 23 °C and 50 °C, θ was reduced to 57±2° and 46±2°, respectively (Figure 5). Thus θ decreased with increasing immersion temperature and time, consistent with literature data [23]. However, silica particle size (5 and 25 nm) had no effect on θ reduction, consistent with Kulak et al. [79] and Costa et al. [80] results for 10-35 nm SiO_2 nanoparticles. Consequently, all subsequent measurements were based on a single particle size only (5nm).

3.4. Effect of temperature on contact angle

Temperature has a major effect on wettability alteration of solid surfaces [35, 51, 52]. Thus, two sets of measurements were performed to examine the effect of temperature on nanofluid wettability alteration efficiency. In the first set (A), immersion temperature was maintained constant at 23°C and contact angles were measured at elevated in-situ temperature. In the second set (B), the temperature for nanofluid treatment and contact angle measurements were the same which is more realistic in oil production application.

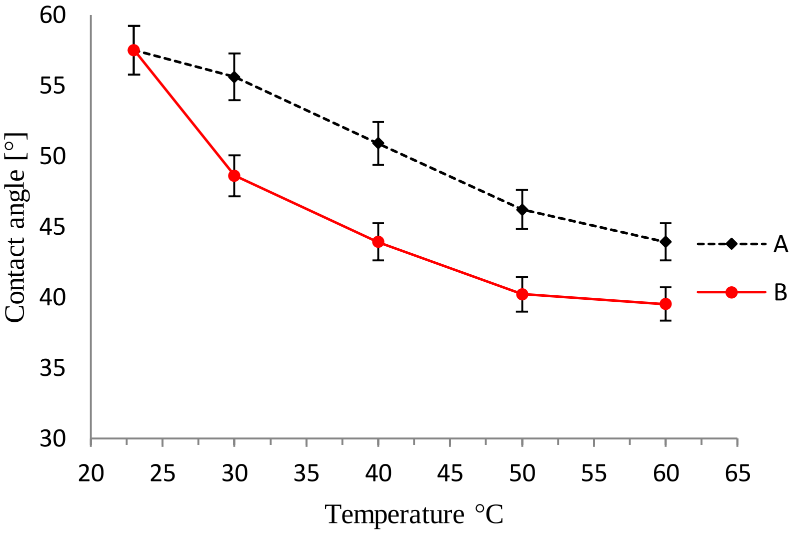

Fig. 6. Advancing water contact angle on oil-wet calcite surface in n-decane after modification with nanofluid for 2 h (0.2wt% SiO2, 1wt% NaCl brine) as a function of measurement temperature. (A) Immersion temperature 23°C. (B) nano-treatment and contact angle measurement temperature were identical.

We found that the efficiency of nanoparticles in terms of reducing the water contact angle significantly improves as temperature increases. For test case A, the contact angle at 23°C reduced from θ = 145° to 56 ° after immersion for 2 hours at 60°C, consistent with our previous study [23]. If the temperature was increased to 60°C during θ measurement, the contact angle reduced further to 43°. This reduction in θ is attributed to the influence of temperature on the spreading behaviour of the drop since the number of active Ca^{+2} sites on the carbonate surface are reduced with increasing temperature [35, 68].

Meanwhile, for test case B, the calcite samples were immersed in nanofluid for 2 h at various elevated temperatures and θ was measured at the same temperatures. In this case at 50 °C, θ was reduced from 145° to 38 ° indicating a significantly higher wettability alteration efficiency. Adhesion of particles on a surface depends on both surfaces charges and surface roughness [70]. These factors control the interaction between silica nanoparticles and carbonate surface since roughness and potential difference can increase the adhesion forces. Mechanistically, more nanoparticles adsorbed onto the limestone surface as temperature increased due to carbonate surface dissolution which increases the surface roughness consistent with EDS results (Table 2). However, when the immersion temperature increased from 50 °C to 60 °C, there was no additional significant influence on θ; which is attributed to the change in surface charge of calcite over 60°C. Zeta potential measurements of calcite surface as function of temperature [68] revealed a reduction in calcite surface charge to a less positive value at higher temperature reducing the difference in surfaces potential

Furthermore, the influence of immersion time on θ was measured for these two test set (Figure 7).

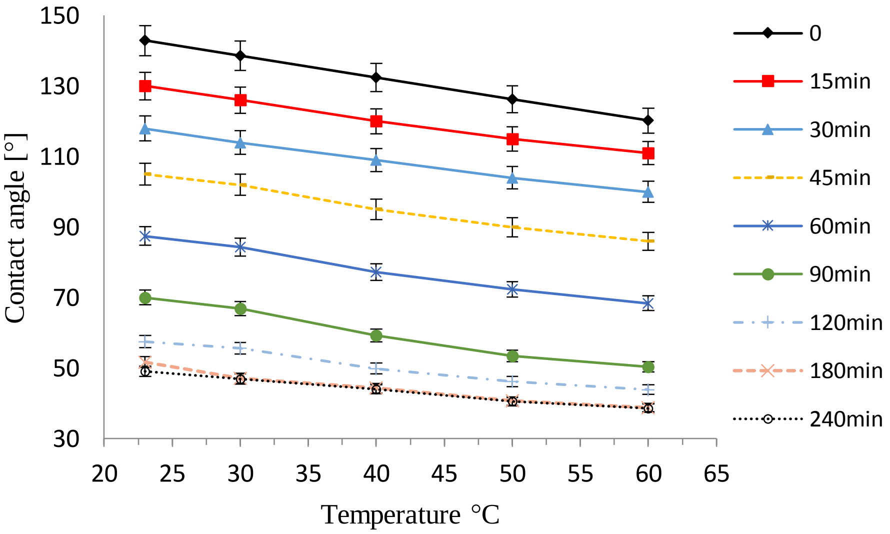

Fig. 7. Set A: advancing water contact angle on oil-wet calcite surface in n-decane as function of exposure time to nanofluid (0.2wt % SiO_2, 2wt % NaCl brine) and temperature. Immersion temperature was constant (23°C).

The contact angle decreased with increasing temperature or immersion time. As wettability alteration of the surface is caused by the continuing adsorption of nanoparticles (see above), longer contact time led to lower θ. However, after 180 min, no more incremental reduction in θ was noticed implying that the surface reached its adsorption capacity [23].

It was proposed that temperature influences the drop behaviour [81], and surface properties [68] which potentially influence the adsorption of silica nanoparticle on a calcite surface [70]. Thus, to distinguish between the two effects, another set of experiments was performed (Figure 8) where both immersion and contact angle measurement conducted at the same elevated temperature. The difference in θ values between the two sets refers to the influence of temperature on nano-silica adsorption.

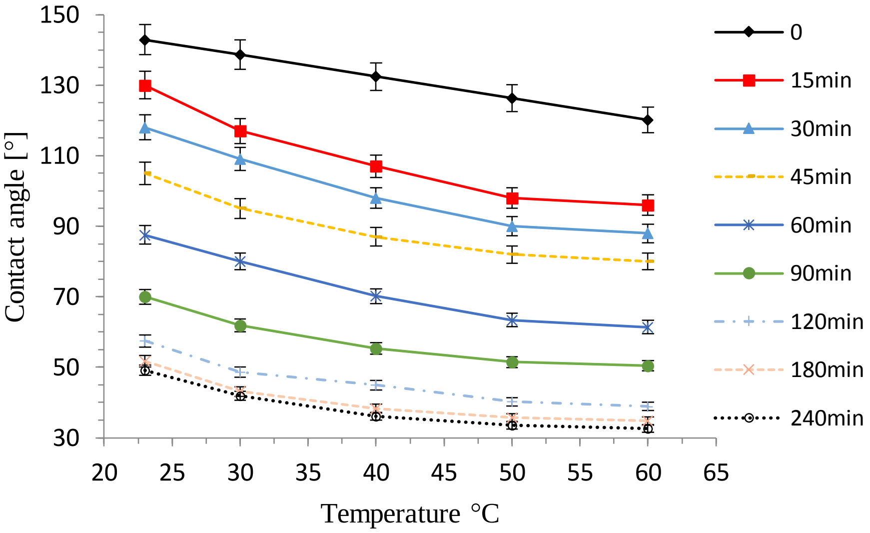

Fig. 8. Set B: advancing water contact angle on oil-wet calcite surface in n-decane as a function of exposure time to nanofluid (0.2 wt% SiO_2, 2 wt% NaCl brine) and temperature. Immersion temperature was the same as the temperature for contact angle measurements.

A clear difference is evident between the two temperatures exposure scenarios (Figure 7 and 8) showing more reduction in set B For instance, after 2 h treatment, θ values measured at 40 °C were 49° and 41° for set A and set B, respectively. Similarly, for each contact angle measurement temperature, all θ values in set B were smaller than those in set A; this difference indicates an increased in particle adsorption with increasing temperature. However, the effect of increasing temperature on contact angle (even up to 60°C) is less considerable as compared to the impact of immersing time for both scenarios (Figures 7, and 8). It is evident that the maximum reduction in contact angle with increasing temperature was at low immersing time (reduction of 20° in θ) and the decrease in θ was less significant at higher immersing times (Figure 8). However, increased immersing time has a more dramatic impacts on contact angle reduction (θ reduced by around 55° and 85° after 1 and 2 hr respectively) consistent with the reported data about the dominant effect of immersing time on nano-treatment efficiency [23, 31, 34, 43]. Mechanistically, the increased temperature effects the surface modification in two different ways: a) it can support nanoparticles adhesion on surface due to increase in surface roughness [70], and b) it leads to a reduction in decrease the adsorption of nanoparticles particularly at temperatures ≥ 50°C due to a reduction in positive charges on calcite surface. Hamouda and Gomari [68] reported that the rise in temperature from 20 °C to 50 °C changed the zeta potential of calcite to a less positive value by 2.5 mV (from 3 mV to 0.5 mV respectively), which in turn decreased the electromotive force (charge difference) for silica particle adsorption; which cause the lower θ in set B.

4. Conclusions

A wettability change from oil-wet to water-wet can enhance oil recovery, particularly in fractured oil-wet limestone [23, 27, 38-43], and it can enhance CO_2 geo-storage capacities [46-48].

It has been previously shown that nanofluids can achieve such a wettability modification [23, 24, 26, 27, 34, 42, 43, 82]. However, there is a series lack of information in terms of how temperature and nanoparticles size influences such a wettability alteration. We thus tested the efficiency of various silica nanofluids in this respect.

Moreover, as a crucial parameter for nanofluid stability, zeta potentials [54, 72, 74] of the different nanofluids were measured at different pH value, particle loads, and salinities.

The results showed that a temperature increase reduces the required immersion time to achieve the same θ reduction. However, at relatively longer immersion periods (≥ 60 min), θ converged to a minimum, independent of temperature. This is caused by an increased adsorption of silica nanoparticles on the calcite surface with increasing temperature, consistent with measurement for Zirconium Oxide nanoparticles [41].

Nanoparticle size (5 or 25 nm), however, had no effect on nanofluid wettability alteration efficiency. All tested nanofluids were stable against agglomeration and sedimentation when the pH of the fluid was kept between 5-6, consistent with Franks [76], Costa et al. [80], Amiri et al. [53] and Al-Anssari et al. [83].

Overall, we conclude that nanofluids are very efficient wettability modifiers, especially at higher temperatures; nanofluids thus have a high potential in the area of enhanced oil recovery and improved CO_2 geo-storage. However, we point out that a comprehensive investigation for zeta potentials of silica nanofluid, oil emulsion, and calcite dispersion at different temperatures is required for much broader understanding of the electrostatic interactions between charged interfaces.

References

[1] Lohse SE, Murphy CJ. Applications of Colloidal Inorganic Nanoparticles: From Medicine to Energy. Journal of the American Chemical Society 2012, 134: 15607-15620

[2] Rubilar O, Rai M, Tortella G, Diez M, Seabra A, Durán N. Biogenic nanoparticles: copper, copper oxides, copper sulphides, complex copper nanostructures and their applications. Biotechnol Lett 2013, 35: 1365-1375

[3] Tong R, Hemmati HD, Langer R, Kohane DS. Photoswitchable Nanoparticles for Triggered Tissue Penetration and Drug Delivery. Journal of the American Chemical Society 2012, 134: 8848-8855

[4] De M, Ghosh PS, Rotello VM. Applications of Nanoparticles in Biology. Advanced Materials 2008, 20: 4225-4241

[5] Baeckkyoung S, Se Hoon K, Sungwoo L, Jaekwan L, Jin-Kyu L, Kwang-Sup S. Nanofluid transport in a living soft microtube. Journal of Physics D: Applied Physics 2015, 48: 345402

[6] Garner K, Keller A. Emerging patterns for engineered nanomaterials in the environment: a review of fate and toxicity studies. Journal of Nanoparticle Research 2014, 16: 1-28

[7] Wu S, Nikolov A, Wasan D. Cleansing dynamics of oily soil using nanofluids. Journal of Colloid and Interface Science 2013, 396: 293-306

[8] Sarkheil H, Tavakoli J. Oil-Polluted Water Treatment Using Nano Size Bagasse Optimized-Isotherm Study. European Online Journal of Natural and Social Sciences 2015, 4: 392-400

[9] Syed S, Alhazzaa MI, Asif M. Treatment of oily water using hydrophobic nano-silica. Chemical Engineering Journal 2011, 167: 99-103

[10] Wang H, Yan N, Li Y, Zhou X, Chen J, Yu B, Gong M, *et al*. Fe nanoparticle-functionalized multi-walled carbon nanotubes: one-pot synthesis and their applications in magnetic removal of heavy metal ions. Journal of Materials Chemistry 2012, 22: 9230-9236

[11] Fischer ARH, van Dijk H, de Jonge J, Rowe G, Frewer LJ. Attitudes and attitudinal ambivalence change towards nanotechnology applied to food production. Public Understanding of Science 2013, 22: 817-831

[12] Rajauria S, Axline C, Gottstein C, Cleland AN. High-Speed Discrimination and Sorting of Submicron Particles Using a Microfluidic Device. Nano Letters 2015, 15: 469-475

[13] van Dijk H, Fischer ARH, Marvin HJP, van Trijp HCM. Determinants of stakeholders' attitudes towards a new technology: nanotechnology applications for food, water, energy and medicine. Journal of Risk Research 2015: 1-22

[14] ShamsiJazeyi H, Miller CA, Wong MS, Tour JM, Verduzco R. Polymer-coated nanoparticles for enhanced oil recovery. Journal of Applied Polymer Science 2014, 131: 1-13

[15] Whitby CP, Fornasiero D, Ralston J. Effect of adding anionic surfactant on the stability of Pickering emulsions. Journal of Colloid and Interface Science 2009, 329: 173-181

[16] Qiao W, Cui Y, Zhu Y, Cai H. Dynamic interfacial tension behaviors between Guerbet betaine surfactants solution and Daqing crude oil. Fuel 2012, 102: 746-750

[17] Ghadimi A, Saidur R, Metselaar HSC. A review of nanofluid stability properties and characterization in stationary conditions. International Journal of Heat and Mass Transfer 2011, 54: 4051-4068

[18] Branson BT, Beauchamp PS, Beam JC, Lukehart CM, Davidson JL. Nanodiamond Nanofluids for Enhanced Thermal Conductivity. ACS Nano 2013, 7: 3183-3189

[19] Winkler K, Paszewski M, Kalwarczyk T, Kalwarczyk E, Wojciechowski T, Gorecka E, Pociecha D, *et al.* Ionic Strength-Controlled Deposition of Charged Nanoparticles on a Solid Substrate. The Journal of Physical Chemistry C 2011, 115: 19096-19103

[20] Chakraborty S, Padhy S. Anomalous Electrical Conductivity of Nanoscale Colloidal Suspensions. ACS Nano 2008, 2: 2029-2036

[21] Balaji T, Yulia B, Atikur R, Saiful I, Mizanur R, Azharul I, Joslyn P, *et al.* Development of Mesoporous Silica Encapsulated Pd-Ni Nanocatalyst for Hydrogen Production. Production and Purification of Ultraclean Transportation Fuels: American Chemical Society 2011: 177-190

[22] Ponmani S, Nagarajan R, Sangwai JS. Effect of Nanofluids of CuO and ZnO in Polyethylene Glycol and Polyvinylpyrrolidone on the Thermal, Electrical, and Filtration-Loss Properties of Water-Based Drilling Fluids. SPE Journal 2015, Preprint

[23] Al-Anssari S, Barifcani A, Wang S, Lebedev M, Iglauer S. Wettability alteration of oil-wet carbonate by silica nanofluid. Journal of Colloid and Interface Science 2016, 461: 435-442

[24] Al-Anssari S, Arif M, Wang S, Barifcani A, Lebedev M, Iglauer S, CO_2 geo-storage capacity enhancement via nanofluid priming, International Journal of Greenhouse Gas Control 2017, 63:20-25

[25] Sharma T, Suresh Kumar G, Sangwai JS. Enhanced oil recovery using oil-in-water (o/w) emulsion stabilized by nanoparticle, surfactant and polymer in the presence of NaCl. Geosystem Engineering 2014, 17: 195-205

[26] Zhang H, Nikolov A, Wasan D. Enhanced Oil Recovery (EOR) Using Nanoparticle Dispersions: Underlying Mechanism and Imbibition Experiments. Energy & Fuels 2014, 28: 3002-3009

[27] Zhang H, Ramakrishnan TS, Nikolov AD, Wasan D. Enhanced Oil Recovery (EOR) Driven by Nanofilm Structural Disjoining Pressure: Flooding Experiments and Microvisualization. Energy & Fuels 2016,

[28] Bayat EA, Junin R, Samsuri A, Piroozian A, Hokmabadi M. Impact of Metal Oxide Nanoparticles on Enhanced Oil Recovery from Limestone Media at Several Temperatures. Energy & Fuels 2014, 28: 6255-6266

[29] Moghaddam N, Rasoul, Bahramian A, Fakhroueian Z, Karimi A, Arya S. Comparative Study of Using Nanoparticles for Enhanced Oil Recovery: Wettability Alteration of Carbonate Rocks. Energy & Fuels 2015, 29: 2111-2119

[30] Täuber D, Trenkmann I, von Borczyskowski C. Influence of van der Waals Interactions on Morphology and Dynamics in Ultrathin Liquid Films at Silicon Oxide Interfaces. Langmuir 2013, 29: 3583-3593

[31] Zhang T, Murphy MJ, Yu H, Bagaria HG, Yoon KY, Nielson BM, Bielawski CW, et al. Investigation of Nanoparticle Adsorption During Transport in Porous Media. SPE Journal 2015, 20: 667-677

[32] Shushan D, Marcoux C. The Rise (and Decline?) of Arab Aid: Generosity and Allocation in the Oil Era. World Development 2011, 39: 1969-1980

[33] Sharma G, Mohanty K. Wettability Alteration in High-Temperature and High-Salinity Carbonate Reservoirs. SPE Journal 2013, 18: 646-655

[34] Roustaei A, Bagherzadeh H. Experimental investigation of SiO_2 nanoparticles on enhanced oil recovery of carbonate reservoirs. J Petrol Explor Prod Technol 2014: 1-7

[35] Gupta R, Mohanty K. Temperature Effects on Surfactant-Aided Imbibition Into Fractured Carbonates. SPE Journal 2010, 25: 80-88

[36] Wu Y, Shuler PJ, Blanco M, Tang Y, Goddard WA. An Experimental Study of Wetting Behavior and Surfactant EOR in Carbonates With Model Compounds. SPE Journal 2008, 13: 26-34

[37] Amraei A, Fakhroueian Z, Bahramian A. Influence of New SiO_2 Nanofluids on Surface Wettability and Interfacial Tension Behaviour between Oil-Water Interface in EOR Processes. Journal of Nano Research 2013, 26: 1-8

[38] Ju B, Fan T. Experimental study and mathematical model of nanoparticle transport in porous media. Powder Technology 2009, 192: 195-202

[39] Onyekonwu MO, Ogolo NA. Investigating the Use of Nanoparticles in Enhancing Oil Recovery. Nigeria Annual International Conference and Exhibitioned. Tinapa - Calabar, Nigeria Society of Petroleum Engineers 2010

[40] Alotaibi MB, Nasralla RA, Nasr-El-Din HA. Wettability Studies Using Low-Salinity Water in Sandstone Reservoirs. 2011,

[41] Karimi A, Fakhroueian Z, Bahramian A, Pour Khiabani N, Darabad JB, Azin R, Arya S. Wettability Alteration in Carbonates using Zirconium Oxide Nanofluids: EOR Implications. Energy & Fuels 2012, 26: 1028-1036

[42] Hendraningrat L, Li S, Torsæter O. A coreflood investigation of nanofluid enhanced oil recovery. Journal of Petroleum Science and Engineering 2013, 111: 128-138

[43] Nwidee LN, Al-Anssari S, Barifcani A, Sarmadivaleh M, Iglauer S. Nanofluids for Enhanced Oil Recovery Processes: Wettability Alteration Using Zirconium Oxide. Offshore Technology Conference Asiaed. Kuala Lumpur, Malaysia: Offshore Technology Conference 2016

[44] Rostami Ravari R, Strand S, Austad T. Combined Surfactant-Enhanced Gravity Drainage (SEGD) of Oil and the Wettability Alteration in Carbonates: The Effect of Rock Permeability and Interfacial Tension (IFT). Energy & Fuels 2011, 25: 2083-2088

[45] Iglauer S, Pentland CH, Busch A. CO_2 wettability of seal and reservoir rocks and the implications for carbon geo-sequestration. Water Resources Research 2015, 51: 729-774

[46] Iglauer S, Al-Yaseri AZ, Rezaee R, Lebedev M. CO_2 wettability of caprocks: Implications for structural storage capacity and containment security. Geophysical Research Letters 2015, 42: 9279-9284

[47] Arif M, Al-Yaseri AZ, Barifcani A, Lebedev M, Iglauer S. Impact of pressure and temperature on CO_2–brine–mica contact angles and CO_2–brine interfacial tension: Implications for carbon geo-sequestration. Journal of Colloid and Interface Science 2016, 462: 208-215

[48] Rahman T, Lebedev M, Barifcani A, Iglauer S. Residual trapping of supercritical CO_2 in oil-wet sandstone. Journal of Colloid and Interface Science 2016, 469: 63-68

[49] Ju B, Fan T, Ma M. Enhanced oil recovery by flooding with hydrophilic nanoparticles. China Particuology 2006, 4: 41-46

[50] Ehtesabi H, Ahadian MM, Taghikhani V, Ghazanfari MH. Enhanced Heavy Oil Recovery in Sandstone Cores Using TiO_2 Nanofluids. Energy & Fuels 2014, 28: 423-430

[51] Al-Sulaimani H, Al-Wahaibi Y, Al-Bahry S, Elshafie A, Al-Bemani A, Joshi S. Residual-Oil Recovery Through Injection of Biosurfactant, Chemical Surfactant, and Mixtures of Both Under Reservoir Temperatures: Induced-Wettability and Interfacial-Tension Effects. 2012,

[52] Chen P, Mohanty KK. Wettability Alteration in High Temperature Carbonate Reservoirs. SPE Improved Oil Recovery Symposiumed. Tulsa, Oklahoma, USA Society of Petroleum Engineers 2014

[53] Amiri A, Øye G, Sjöblom J. Influence of pH, high salinity and particle concentration on stability and rheological properties of aqueous suspensions of fumed silica. Colloids and Surfaces A: Physicochemical and Engineering Aspects 2009, 349: 43-54

[54] Tantra R, Schulze P, Quincey P. Effect of nanoparticle concentration on zeta-potential measurement results and reproducibility. Particuology 2010, 8: 279-285

[55] Li YV, Cathles LM. Retention of silica nanoparticles on calcium carbonate sands immersed in electrolyte solutions. Journal of Colloid and Interface Science 2014, 436: 1-8

[56] Marmur A. Soft contact: measurement and interpretation of contact angles. Soft Matter 2006, 2: 12-17

[57] Munshi AM, Singh VN, Kumar M, Singh JP. Effect of nanoparticle size on sessile droplet contact angle. Journal of Applied Physics 2008, 103

[58] Iglauer S, Salamah A, Sarmadivaleh M, Liu K, Phan C. Contamination of silica surfaces: Impact on water–CO_2–quartz and glass contact angle measurements. International Journal of Greenhouse Gas Control 2014, 22: 325-328

[59] Alroudhan A, Vinogradov J, Jackson MD. Zeta potential of intact natural limestone: Impact of potential-determining ions Ca, Mg and SO4. Colloids and Surfaces A: Physicochemical and Engineering Aspects 2016, 493: 83-98

[60] Lander LM, Siewierski LM, Brittain WJ, Vogler EA. A systematic comparison of contact angle methods. Langmuir 1993, 9: 2237-2239

[61] Hansen G, Hamouda AA, Denoyel R. The effect of pressure on contact angles and wettability in the mica/water/n-decane system and the calcite+stearic acid/water/n-decane system. Colloids and Surfaces A: Physicochemical and Engineering Aspects 2000, 172: 7-16

[62] Mihajlovic S, Sekulic Ž, Dakovic A, Vucinic* D, Jovanovic V, Stojanovic J. Surface Properties of Natural Calcite Filler Treated with Stearic Acid. Ceramics – Silikáty 2009, 53: 268-275

[63] Shi X, Rosa R, Lazzeri A. On the Coating of Precipitated Calcium Carbonate with Stearic Acid in Aqueous Medium. Langmuir 2010, 26: 8474-8482

[64] Morse JW, Arvidson RS. The dissolution kinetics of major sedimentary carbonate minerals. Earth-Science Reviews 2002, 58: 51-84

[65] Hoeiland S, Barth T, Blokhus AM, Skauge A. The effect of crude oil acid fractions on wettability as studied by interfacial tension and contact angles. Journal of Petroleum Science and Engineering 2001, 30: 91-103

[66] Sondi I, Bišćan J, Vdović N, Škapin S.D, The electrokinetic properties of carbonates in aqueous media revisited, Colloids and Surfaces A: Physicochemical and Engineering Aspects, 2009, 342: 84-91.

[67] Heberling F, Trainor T.P, Lützenkirchen J, Eng P, Denecke M.D, Bosbach D, Structure and reactivity of the calcite–water interface, Journal of Colloid and Interface Science, 2011, 354: 843-857.

[68] Hamouda AA, Gomari RKA. Influence of Temperature on Wettability Alteration of Carbonate Reservoirs. SPE/DOE Symposium on Improved Oil Recoveryed. Tulsa, Oklahoma, USA Society of Petroleum Engineers 2006

[69] Gomari RKA, Hamouda AA. Effect of fatty acids, water composition and pH on the wettability alteration of calcite surface. Journal of Petroleum Science and Engineering 2006, 50: 140-150

[70] Israelachvili JN. 17 - Adhesion and Wetting Phenomena. Intermolecular and Surface Forces (Third Edition) San Diego: Academic Press 2011: 415-467

[71] El-sayed GM, Kamel MM, Morsy NS, Taher FA. Encapsulation of nano Disperse Red 60 via modified miniemulsion polymerization. I. Preparation and characterization. Journal of Applied Polymer Science 2012, 125: 1318-1329

[72] Bayat A, Junin R, Ghadikolaei F, Piroozian A. Transport and aggregation of Al_2O_3 nanoparticles through saturated limestone under high ionic strength conditions: measurements and mechanisms. Journal of Nanoparticle Research 2014, 16: 1-12

[73] Dishon M, Zohar O, Sivan U. From Repulsion to Attraction and Back to Repulsion: The Effect of NaCl, KCl, and CsCl on the Force between Silica Surfaces in Aqueous Solution. Langmuir 2009, 25: 2831-2836

[74] Metin C, Lake L, Miranda C, Nguyen Q. Stability of aqueous silica nanoparticle dispersions. Journal of Nanoparticle Research 2011, 13: 839-850

[75] Mondragon R, Julia JE, Barba A, Jarque JC. Characterization of silica–water nanofluids dispersed with an ultrasound probe: A study of their physical properties and stability. Powder Technology 2012, 224: 138-146

[76] Franks GV. Zeta Potentials and Yield Stresses of Silica Suspensions in Concentrated Monovalent Electrolytes: Isoelectric Point Shift and Additional Attraction. Journal of Colloid and Interface Science 2002, 249: 44-51

[77] Wolthers M, Charlet L, Van Cappellen P. The surface chemistry of divalent metal carbonate minerals; a critical assessment of surface charge and potential data using the charge

distribution multi-site ion complexation model. American Journal of Science 2008, 308: 905-941

[78] Nikolov A, Kondiparty K, Wasan D. Nanoparticle Self-Structuring in a Nanofluid Film Spreading on a Solid Surface. Langmuir 2010, 26: 7665-7670

[79] Kulak A, Hall SR, Mann S. Single-step fabrication of drug-encapsulated inorganic microspheres with complex form by sonication-induced nanoparticle assembly. Chemical Communications 2004: 576-577

[80] Costa CAR, Leite CAP, Galembeck F. ESI-TEM Imaging of Surfactants and Ions Sorbed in Stöber Silica Nanoparticles. Langmuir 2006, 22: 7159-7166

[81] de Ruijter M, Kölsch P, Voué M, De Coninck J, Rabe JP. Effect of temperature on the dynamic contact angle. Colloids and Surfaces A: Physicochemical and Engineering Aspects 1998, 144: 235-243

[82] Bayat A, Junin R, Mohsin R, Hokmabadi M, Shamshirband S. Influence of clay particles on Al_2O_3 and TiO_2 nanoparticles transport and retention through limestone porous media: measurements and mechanisms. Journal of Nanoparticle Research 2015, 17: 1-14

[83] Al-Anssari S, Wang S, Barifcani A, Iglauer S, Oil-water interfacial tensions of silica nanoparticle-surfactant formulations, Tenside Surfactants Detergents, In press (2017).